Reprinted from **Applied Optics,** Vol. 20, page 3635, October 15, 1981

Heterodyne frequency measurements of $^{13}CO_2$ laser hot band transitions

F. R. Petersen, J. S. Wells, A. G. Maki, and K. J. Siemsen

The frequencies of twenty-eight lines in the P-branch of the 01^11-$[11^10, 03^10]_{\mathrm{I}}$ band of $^{13}C^{16}O_2$, observed in laser emission, and three lines in the R-branch, observed in absorption with a diode laser, have been carefully measured with stabilized CO_2 lasers. A significant improvement in the ro-vibrational constants has been obtained from a least squares fit to these data. The laser lines stabilized by saturated absorption techniques provide convenient, accurate (uncertainty <0.1 MHz) frequency references near 11.7 μm.

I. Introduction

The CO_2 laser, with its many isotopic species and lines with accurately determined frequencies, has developed into an extremely useful frequency and wavelength standard in the 9–12-μm spectral region.[1,2] Recent heterodyne diode laser spectroscopic experiments on molecules such as OCS (carbonyl sulfide), with a CO_2 laser stabilized on a Doppler-free absorption feature as the reference, have extended the usefulness of CO_2 for calibration work.[3] Because of the limited bandpass of currently used detectors, these heterodyne experiments require CO_2 calibration lines within a few gigahertz of the molecular line to be measured. A need for calibration lines at $\lambda > 11.6$ μm motivated interest in the 01^11-$[11^10, 03^10]_{\mathrm{I}}$ band of $^{13}CO_2$.[4] Standing wave saturation resonances can be observed in a low-pressure room-temperature absorption cell for these laser lines.[5,6] Since the frequencies were not known with great accuracy, an experiment was undertaken to improve this situation.

The line frequencies of the normal laser bands of $^{12}C^{16}O_2$ stabilized by saturated absorption are known to within a few tens of kilohertz relative to the cesium standard. The frequencies of other IR lasers can be accurately synthesized and measured with these known CO_2 laser lines in heterodyne-type experiments.[7,8] The measurement here follows that technique.

II. Experimental

In the 01^11-$[11^10, 03^10]_{\mathrm{I}}$ band of $^{13}CO_2$, laser oscillation occurred only on lines in the P-branch. Most of the experimental data, therefore, was taken here. Because of problems associated with fitting constants to data taken in only one branch, a few tunable diode laser (TDL) heterodyne measurements were done in the R-branch. Most of the measurements were done at the National Bureau of Standards. Lines $P(9)$ and $P(31)$–$P(39)$, however, were done at the National Research Council with a higher gain, lower loss CO_2 laser.

Figure 1 shows the experimental arrangement for the P-branch measurements. At NBS, the hot band laser, ν_3, was 2 m long with a 4-m radius, 98% reflectivity coupling mirror and a 150-line/mm Au coated grating for line selection. The dc discharge tube (178 cm long) was filled with a mixture of 40 Pa H_2, 187 Pa 90% isotopically pure $^{13}C^{16}O_2$, 187 Pa N_2, and 360 Pa He. The standing wave saturation resonance was observed with the 4.3-μm fluorescent radiation[5] by sending the external beam through a low-pressure (4.0–5.3-Pa) absorption cell and reflecting it back nearly upon itself. The slight angular divergence (~2 mrad) between the incident and reflected beam allowed the full reflected beam to be sent to a W-Ni point-contact diode. Even though the lower laser level is 2037 cm^{-1} (band center) above the ground state, the saturation resonance could still be observed at room temperature (~300 K), although the intensity was lower than for the normal laser bands. Figure 2 shows a recording for $P(21)$ as observed with a lock-in amplifier. For each measurement, the frequency of the hot band laser was set to a value corresponding to the intensity minimum in the saturation dip.

For lines $P(10)$–$P(30)$, measured at NBS, the unknown $^{13}CO_2$ frequency was synthesized by two $^{12}CO_2$

K. J. Siemsen is with National Research Council of Canada, Ottawa K1A OR6; A. G. Maki is with U.S. National Bureau of Standards, Molecular Spectroscopy Division, Washington, D.C. 20234; the other authors are with U.S. National Bureau of Standards, Time & Frequency Division, Boulder, Colorado 80303.

Received 9 May 1981.

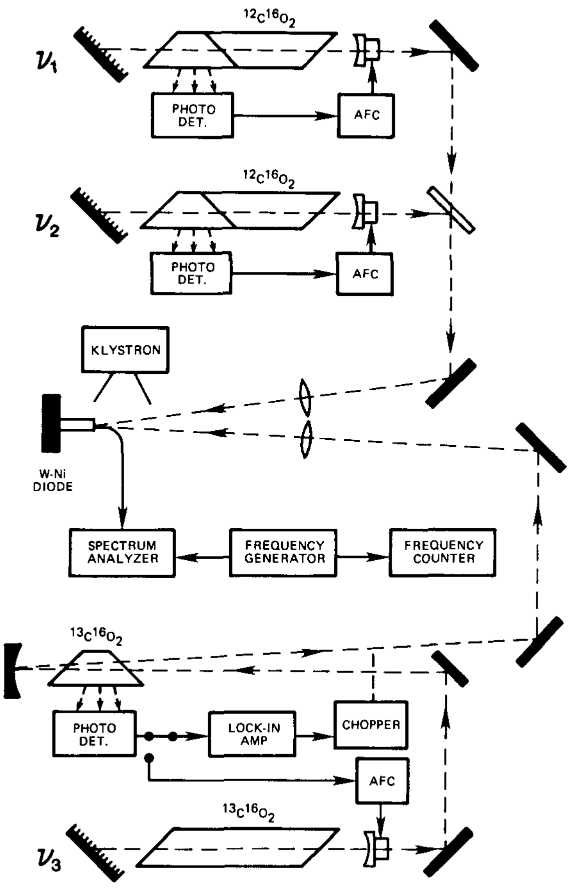

Fig. 1. Schematic diagram of the heterodyne experiment to measure frequencies of lasing 01^11–$[11^10, 03^10]_I$ $^{13}CO_2$ transitions. The unknown frequency, ν_3, was synthesized as $\nu_3 = 2\nu_2 - \nu_1 \pm m\nu_{\mu w} \pm \nu_B$, where ν_1, ν_2, and ν_3 were the laser frequencies indicated in the diagram, $\nu_{\mu w}$ was an X-band klystron frequency with $m = 0$ or 1, and ν_B was the observed beat frequency.

lasers, ν_1 and ν_2, with the harmonic combination $2\nu_2 - \nu_1$. An X-band klystron was used in cases where the difference between the $^{12}CO_2$ synthesized frequency and the unknown $^{13}CO_2$ frequency exceeded the bandpass of the receiver system. The two $^{12}CO_2$ synthesis lasers were frequency locked to the standing wave saturation resonances observed in fluorescence with intracavity $^{12}CO_2$ absorption cells filled to a pressure of 5.3 Pa. The phase and amplitude of the frequency modulation of one synthesis laser were adjusted relative to that of the other to minimize the width of the beat note as observed on a spectrum analyzer. The beat frequency was measured by setting a marker from a frequency synthesizer to the center of the beat note. Typically, ten measurements were taken for each $^{13}CO_2$ laser line; each time the laser intensity was carefully set to the bottom of the absorption dip by changing the laser frequency. The standard deviation for each group of ten measurements was ~0.1 MHz. The results are summarized in Table I.

The remaining measurements in the P-branch, i.e., $P(9)$ and $P(31)$–$P(39)$, were done at NRC by a technique similar to that just described. In this case, the hot band laser, ν_3, was the laser described by Siemsen.[9] It was filled to a total pressure of 1.31 kPa with a mixture of Xe, $^{13}CO_2$, N_2, and He in the ratio 1:1:2:6. For each measurement, ν_3 was set to a frequency corresponding to the peak of the laser gain curve. The frequency of each reference laser was set to the zero-slope point in the 4.3-μm saturation dip as observed with a lock-in amplifier. The CO_2 pressure in the intracavity absorption cells of ν_1 and ν_2, each raised to a temperature from 390 to 420 K, was 15 Pa. The beat frequency was observed on a spectrum analyzer and measured with a frequency generator and counter. For each line, five measurements were taken. The standard deviation for each group was ~0.7 MHz. The results are given in Table I.

The R-branch measurements, also shown in Table I, were made with a TDL heterodyne technique.[3,4] Because of detector bandpass considerations, only R-branch hot band lines within a few gigahertz of normal laser band reference lines were selected. The diode laser was either frequency locked or manually tuned to the R-branch absorption line center. Its beat frequency with a stabilized $^{13}CO_2$ reference laser was obtained with a HgCdTe photovoltaic detector and measured with a spectrum analyzer and signal averager. As before, pressure in the reference laser absorption cell was 5.3 Pa. The 2-m long, hot band absorption cell was filled to 1.3 kPa with 90% isotopically pure $^{13}C^{16}O_2$ and then heated to ~470 K to enhance the absorption signal. The 3-MHz uncertainty assigned to each measurement arises from the Doppler width of the absorption line and

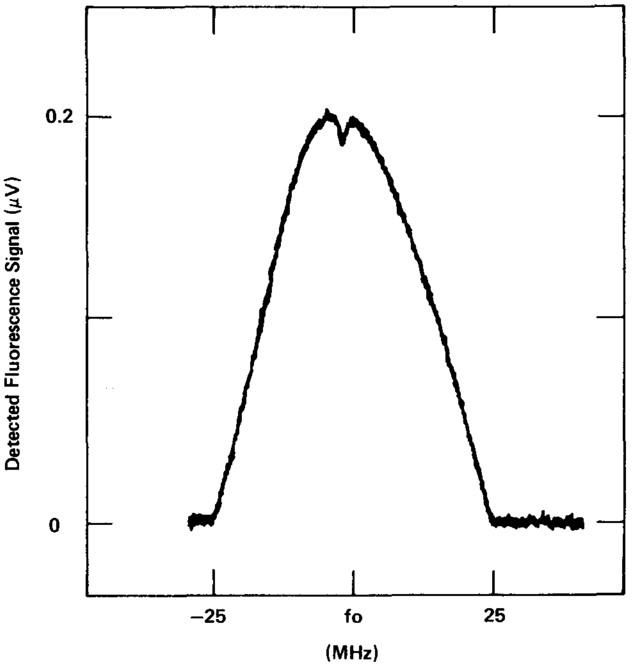

Fig. 2. Fluorescent signal observed from a room temperature external absorption cell filled with 5.3-Pa $^{13}CO_2$ as the frequency ν_3 was swept across the gain curve of $P(21)$ in the 01^11–$[11^10, 03^10]_I$ band of $^{13}CO_2$. Laser power was about 1 W, and the bandpass of the lock-in amplifier was 0.4 Hz.

Table I. Summary of $^{13}CO_2$ 01^11–$[11^10, 03^10]_I$ Frequencies Measured by the Heterodyne Technique [a]

J	Ref. freq. $^{12}C^{16}O_2$ * $^{13}C^{16}O_2$	Observed diff. Hot–Ref. (MHz)	01^11–$[11^10, 03^10]_I$ Obs. freq., $^{13}C^{16}O_2$ (MHz)[b]	Residual Obs.–Calc. (MHz)[c]
P-branch				
39	$2P_I(22)$–$P_{II}(32)$	−2 168.38	25 458 996.92 (100)	−1.30
38	$2R_I(4)$–$R_{II}(22)$	1 850.07	25 474 786.76 (100)	−2.52
37	$2R_I(12)$–$R_{II}(40)$	2 073.36	25 516 393.80 (100)	−0.38
36	$2P_I(24)$–$P_{II}(38)$	1 228.50	25 533 176.26 (100)	−1.60
35	$2P_I(44)$–R_I (42)	576.77	25 573 221.78 (100)	0.58
34	$2R_I(10)$–$R_{II}(30)$	−674.50	25 590 927.31 (100)	0.19
33	$2R_I(4)$–$R_{II}(14)$	479.67	25 629 481.29 (100)	1.27
32	$2R_I(8)$–$R_{II}(22)$	−1 070.82	25 648 039.03 (100)	0.20
31	$2R_I(8)$–$R_{II}(20)$	−1 760.61	25 685 171.38 (100)	0.10
30	$2P_I(10)$–$P_{II}(18)$	−9 276.510	25 704 514.694 (54)	0.049
29	$2P_I(8)$–$P_{II}(16)$	−1 350.553	25 740 295.567 (45)	−0.002
28	$2P_I(10)$–$P_{II}(20)$	10 958.094	25 760 356.050 (51)	0.012
27	$2P_I(8)$–$P_{II}(18)$	−169.889	25 794 853.442 (55)	0.077
26	$2P_I(12)$–$P_{II}(26)$	272.377	25 815 564.358 (52)	−0.002
25	$2P_I(8)$–$P_{II}(20)$	−338.077	25 848 845.025 (40)	−0.054
24	$2P_I(10)$–$P_{II}(24)$	10 089.550	25 870 140.759 (39)	−0.053
23	$2R_I(14)$–$R_{II}(22)$	−44.969	25 902 271.035 (46)	0.003
22	$2R_I(12)$–$R_{II}(16)$	−11 158.958	25 924 086.474 (50)	0.026
21	$2R_I(18)$–$R_{II}(28)$	146.740	25 955 131.481 (49)	0.018
20	$2R_I(14)$–$R_{II}(18)$	−1 352.977	25 977 402.181 (44)	−0.002
19	$2P_I(14)$–$P_{II}(36)$	994.544	26 007 426.521 (38)	−0.009
17	$2R_I(14)$–$R_{II}(14)$	775.378	26 059 156.317 (41)	0.013
16	$2P_I(8)$–$P_{II}(28)$	8 571.544	26 082 146.885 (48)	0.017
15	$2R_I(22)$–$R_{II}(28)$	−75.338	26 110 320.772 (42)	−0.003
14	$2R_I(22)$–$R_{II}(26)$	−12 270.819	26 133 576.959 (47)	0.039
12	$2R_I(14)$–$R_{II}(8)$	559.682	26 184 379.237 (35)	−0.034
10	$2P_I(36)$–$R_I(32)$	9 230.921	26 234 554.149 (56)	0.038
9	$2R_I(26)$–$R_{II}(28)$	637.37	26 260 420.02 (100)	−0.995
R-branch				
18	$P_I(20)$*	2 626.6	26 891 296.3 (30)	−2.6
23	$P_I(16)$*	1 976.8	26 994 349.8 (30)	−2.2
34	$P_I(8)$*	3 249.7	27 196 009.9 (30)	0.6

[a] For laser lines $P(9)$ and $P(31)$–$P(39)$, the $^{13}CO_2$ frequency was set to the peak of the gain curve. Other laser line frequencies in the P-branch were set to the minimum in the saturation dip. Lines in the R-branch were observed in absorption with a TDL which was set to the absorption maximum. All reference lasers were stabilized to standing wave saturation resonances in CO_2.

[b] Number in parentheses is the estimated uncertainty in the measured frequency. For lines $P(10)$–$P(30)$, it is the 1-σ estimated uncertainty in the synthesized frequency and the $\sigma_{\bar{x}}$ of the measured frequency combined in quadrature. For lines in the R-branch, the uncertainty is estimated from the width of the beat note and the Doppler width and SNR of the absorption line.

[c] Frequencies were calculated with the ro-vibrational constants from the fit without the H terms.

the width of the beat note. Because of detector bandpass and TDL limitations, only three lines could be measured in this manner.

III. Assignment and Analysis

The band center for the 01^11–$[11^10, 03^10]_I$ band was estimated to be $\nu_0 = 883.15$ cm^{-1} by using the band center data given in Refs. 10–12 for $\nu_0(01^11\text{–}01^10) = 2271.76$ cm^{-1}, $\nu_0(01^10\text{–}00^00) = 648.48$ cm^{-1}, and $\nu_0([11^10, 03^10]_I\text{–}00^00) = 2037.09$ cm^{-1}. With this tentative band center and the constants given in Ref. 10, the J-numbering of the observed transitions could be tentatively estimated. The identification of the laser transitions was finally confirmed by observing that the upper and lower state constants resulting from the least squares fit of the laser transitions were in excellent agreement with the constants given by Baldacci *et al.*[10]

The heterodyne measurements were analyzed by using a double-precision (72 binary bits) least squares program, ORTHO, developed by Philip Walsh of NBS. This program uses a Gram-Schmidt orthonormalization technique that is superior to many other least squares algorithms.[13] The measurements from both NBS and NRC were combined by weighting each datum by the reciprocal of the square of its estimated uncertainty. The NBS and NRC data were assigned uncertainties in locating the laser line centers that are given in parentheses in Table I. These uncertainties are confirmed from the residuals calculated from the least squares fit.

The data were fit to the usual equations for the CO_2 energy levels:

$$\begin{aligned}\nu_{\text{obs}} = {} & \nu_0 + B'J'(J'+1) - B''J''(J''+1) - D'[J'(J'+1)-1]^2 \\ & + D''[J''(J''+1)-1]^2 + H'[J'(J'+1)-1]^3 \\ & - H''[J''(J''+1)-1]^3 \\ & \pm \tfrac{1}{2}\{q'J'(J'+1) - q''J''(J''+1) \\ & - \mu'[J'(J'+1)]^2 + \mu''[J''(J''+1)]^2\}, \qquad (1)\end{aligned}$$

where the upper sign for the splitting term was used for the f levels (even values of J''), and the lower sign was used for the e levels (odd values of J'').

Table II. Ro-vibrational constants for the 01^11–$[11^10, 03^10]_{\mathrm{I}}$ Band of $^{13}\mathrm{C}^{16}\mathrm{O}_2$

	Fit without H'		Fit with H'	
Constant	(MHz)[a]	(cm^{-1})[b]	(MHz)[a]	(cm^{-1})[b]
ν_0	26 476 012.149(249)	883.144 703 4	26 476 011.391(320)	883.144 678 4
B'	11 631.573 9(158)	0.387 987 542	11 631.507 7(243)	0.387 985 334
D'	$4.080\,67(837) \times 10^{-3}$	$1.361\,16 \times 10^{-7}$	$4.039\,21(1440) \times 10^{-3}$	$1.347\,34 \times 10^{-7}$
$(H'\text{–}H'')$[c]	[0.0]		$-3.336(978) \times 10^{-9}$	-1.113×10^{-13}
q'	18.403 52(830)	$6.138\,754 \times 10^{-4}$	18.402 41(767)	$6.138\,383 \times 10^{-4}$
μ'	$2.79(135) \times 10^{-5}$	9.31×10^{-10}	$3.74(128) \times 10^{-5}$	12.48×10^{-10}
B''	11 706.458 3(149)	0.390 485 417	11 706.396 9(227)	0.390 483 369
D''	$3.784\,08(765) \times 10^{-3}$	$1.262\,23 \times 10^{-7}$	$3.751\,78(1182) \times 10^{-3}$	$1.251\,46 \times 10^{-7}$
q''	25.984 72(703)	$8.667\,570 \times 10^{-4}$	25.984 14(650)	$8.667\,376 \times 10^{-4}$
μ''	$-1.315(127) \times 10^{-4}$	-4.386×10^{-9}	$-1.228(120) \times 10^{-4}$	-4.096×10^{-9}

[a] Uncertainty in the last digits (one estimated standard error) is given in parentheses.

[b] $c = 299\,792\,458$ m/sec.[14]

[c] Fitting H' alone gives a better approximation to the value of H'–H'' rather than to H' alone.

Table III. Variance-Covariance Matrix (in units of MHz^2) for the Constants Given in Table II (Without the H Terms)

	ν_0	B'	D'	q'	μ'	B''	D''	q''	μ''
ν_0	6.19634×10^{-2}	3.81243×10^{-3}	1.23631×10^{-6}	7.58418×10^{-4}	3.21301×10^{-7}	3.62650×10^{-3}	1.07378×10^{-6}	6.83929×10^{-4}	2.52226×10^{-7}
B'		2.49503×10^{-4}	6.31490×10^{-8}	3.00904×10^{-5}	3.66665×10^{-8}	2.35627×10^{-4}	5.31320×10^{-8}	2.82634×10^{-5}	3.21583×10^{-8}
D'			6.99841×10^{-11}	3.19308×10^{-8}	-4.30197×10^{-11}	6.29620×10^{-8}	6.39580×10^{-11}	2.62703×10^{-8}	-4.15322×10^{-11}
q'				6.88183×10^{-5}	-4.73735×10^{-8}	3.05629×10^{-5}	2.96891×10^{-8}	5.81902×10^{-5}	-4.83105×10^{-8}
μ'					1.82935×10^{-10}	3.15223×10^{-8}	-4.09967×10^{-11}	-3.36912×10^{-8}	1.71443×10^{-10}
B''						2.22769×10^{-4}	5.33249×10^{-8}	2.84439×10^{-5}	2.73754×10^{-8}
D''							5.85956×10^{-11}	2.43775×10^{-8}	-3.95425×10^{-11}
q''								4.94904×10^{-5}	-3.49741×10^{-8}
μ''									1.60978×10^{-10}

Although the $^{13}\mathrm{CO}_2$ laser line measurements are very precise, they include only P-branch transitions and extend from $J'' = 9$ to $J'' = 39$, a limited range of J values compared with what is possible in absorption or spontaneous emission measurements. To improve the accuracy of any calculated transitions, efforts were made to measure some R-branch transitions. For reasons mentioned before, only $R(18)$, $R(23)$, and $R(34)$ could be measured by the TDL heterodyne technique. Even with these three R-branch measurements, the data were not capable of determining both μ terms and both H terms in Eq. (1).

Fortunately Baldacci *et al.*[10] have reported IR grating measurements on the 01^11–01^10 band and the $[11^11, 03^11]_{\mathrm{I}}$–$[11^10, 03^10]_{\mathrm{I}}$ band (which they labeled the 11^11–11^10 band) from which we have extracted high J combination differences for both the 01^11 and $[11^10, 03^10]_{\mathrm{I}}$ states, the upper and lower states of the laser transitions. The combination differences were included in the least squares fit with uncertainties of ±180 MHz for the $[11^10, 03^10]_{\mathrm{I}}$ state and ±150 MHz for the 01^11 state. Since these combination differences extended to $J = 83$ for the 01^11 state and to $J = 56$ for the $[11^10, 03^10]_{\mathrm{I}}$ state, their inclusion significantly reduced the uncertainty of the derived constants and particularly of the calculated high J transitions in spite of the large uncertainty assigned to the combination differences.

Even with the inclusion of the combination differences, however, the values of μ' and H' are about equal to three times their estimated standard error. This result means that it is not certain whether the values determined for μ' and H' are realistic, or whether they are just artifacts resulting from experimental errors. In cases such as this, it is always difficult to decide if these constants should be evaluated in the least squares fit or omitted. Since the value obtained for H'' was approximately equal to its uncertainty, it was clear that H'' could not be determined by the data and was, consequently, omitted from the fits reported in Table II.

In Table II, two sets of constants are given for the 01^11–$[11^10, 03^10]_{\mathrm{I}}$ band. One set includes the μ' term, while the other set includes both the μ' and H' terms. Since the H'' term was not determinable and therefore was effectively set equal to zero, the value obtained for H' is more properly ascribed to a value for H'–H'' (as is indicated in Table II).

Table III gives the variance–covariance matrix for the constants determined without the H terms. For con-

Table IV. Frequencies and Wave Numbers for the 01^11-$[11^10, 03^10]_{\mathrm{I}}$ Band of $^{13}CO_2$ Calculated with the Ro-vibrational Constants from Table II (without the H terms)

Rot. trans.	Wave number (cm^{-1})[a]	Frequency (MHz)[a]	Rot. trans.	Wave number (cm^{-1})[a]	Frequency (MHz)[a]
$P(50)$	837.609940(64)	25110914.276(1909)	$R(1)$	884.690680(10)	26522359.352(307)
$P(49)$	839.362427(55)	25163452.505(1658)	$R(2)$	885.458711(12)	26545384.349(356)
$P(48)$	839.687042(50)	25173184.219(1500)	$R(3)$	886.217658(12)	26568137.000(372)
$P(47)$	841.372307(43)	25223707.197(1300)	$R(4)$	886.975092(15)	26590844.300(435)
$P(46)$	841.742361(39)	25234801.135(1157)	$R(5)$	887.725608(15)	26613344.206(446)
$P(45)$	843.363044(33)	25283388.000(1001)	$R(6)$	888.470400(17)	26635672.514(520)
$P(44)$	843.775986(29)	25295767.670(874)	$R(7)$	889.214498(18)	26657980.003(528)
$P(43)$	845.334677(25)	25342496.069(755)	$R(8)$	889.944596(20)	26679867.807(608)
$P(42)$	845.787999(21)	25356086.324(643)	$R(9)$	890.684293(21)	26702043.339(622)
$P(41)$	847.287242(19)	25401032.476(555)	$R(10)$	891.397637(23)	26723428.851(700)
$P(40)$	847.778481(15)	25415759.456(459)	$R(11)$	892.134954(24)	26745533.080(728)
$P(39)$	849.220770(13)	25458998.211(395)	$R(12)$	892.829471(26)	26766354.173(792)
$P(38)$	849.747504(11)	25474789.277(315)	$R(13)$	893.566442(28)	26788448.007(850)
$P(37)$	851.135294(9)	25516394.177(271)	$R(14)$	894.240046(30)	26808642.157(885)
$P(36)$	851.695137(7)	25533177.855(206)	$R(15)$	894.978713(33)	26830786.820(992)
$P(35)$	853.030839(6)	25573221.199(177)	$R(16)$	895.629304(33)	26850291.041(979)
$P(34)$	853.621445(4)	25590927.113(127)	$R(17)$	896.371720(39)	26872548.133(1159)
$P(33)$	854.907431(4)	25629480.014(109)	$R(18)$	896.997179(36)	26891298.919(1072)
$P(32)$	855.526487(2)	25648038.830(72)	$R(19)$	897.745416(45)	26913730.480(1356)
$P(31)$	856.765092(2)	25685171.278(62)	$R(20)$	898.343605(39)	26931663.740(1167)
$P(30)$	857.410317(1)	25704514.640(39)	$R(21)$	899.099747(53)	26954332.308(1589)
$P(29)$	858.603840(1)	25740295.564(33)	$R(22)$	899.668507(42)	26971383.309(1267)
$P(28)$	859.272985(1)	25760356.034(24)	$R(23)$	900.434659(62)	26994351.983(1865)
$P(27)$	860.423692(1)	25794853.362(22)	$R(24)$	900.971808(46)	27010455.287(1377)
$P(26)$	861.114537(1)	25815564.357(21)	$R(25)$	901.750096(73)	27033787.788(2192)
$P(25)$	862.224662(1)	25848845.075(21)	$R(26)$	902.253425(50)	27048877.189(1503)
$P(24)$	862.935011(1)	25870140.808(21)	$R(27)$	903.045997(86)	27072637.922(2577)
$P(23)$	864.006760(1)	25902271.029(20)	$R(28)$	903.513269(55)	27086646.387(1656)
$P(22)$	864.734444(1)	25924086.446(20)	$R(29)$	904.322300(101)	27110900.501(3027)
$P(21)$	865.769994(1)	25955131.461(18)	$R(30)$	904.751250(62)	27123760.107(1847)
$P(20)$	866.512865(1)	25977402.180(20)	$R(31)$	905.578937(118)	27148573.557(3552)
$P(19)$	867.514370(1)	26007426.528(18)	$R(32)$	905.967269(70)	27160215.432(2089)
$P(18)$	868.270301(1)	26030088.780(21)	$R(33)$	906.815843(139)	27185655.039(4159)
$P(17)$	869.239889(1)	26059156.302(20)	$R(34)$	907.161224(80)	27196009.301(2394)
$P(16)$	870.006772(1)	26082146.866(21)	$R(35)$	908.032944(162)	27222142.814(4856)
$P(15)$	870.946552(1)	26110320.773(28)	$R(36)$	908.333008(93)	27231138.505(2775)
$P(14)$	871.722294(1)	26133576.918(20)	$R(37)$	909.230167(189)	27258034.663(5653)
$P(13)$	872.634356(1)	26160919.848(39)	$R(38)$	909.482509(108)	27265599.695(3242)
$P(12)$	873.416878(1)	26184379.270(22)	$R(39)$	910.407436(219)	27293328.288(6559)
$P(11)$	874.303294(2)	26210953.348(55)	$R(40)$	910.609612(127)	27299389.374(3806)
$P(10)$	875.090530(1)	26234554.110(33)	$R(41)$	911.564670(253)	27328021.302(7584)
$P(9)$	875.953358(3)	26260421.015(76)	$R(42)$	911.714193(149)	27332503.902(4475)
$P(8)$	876.743253(2)	26284101.484(57)	$R(43)$	912.701788(291)	27362111.241(8736)
$P(7)$	877.584536(3)	26309322.503(103)	$R(44)$	912.796128(175)	27364939.495(5260)
$P(6)$	878.375042(3)	26333021.291(91)	$R(45)$	913.818704(334)	27395595.552(****)
$P(5)$	879.196814(5)	26357657.387(136)	$R(46)$	913.855285(206)	27396692.223(6167)
$P(4)$	879.985890(4)	26381313.287(134)	$R(47)$	914.915331(382)	27428471.603(****)
$P(3)$	880.790175(6)	26405425.156(176)	$R(48)$	914.891529(240)	27427758.013(7208)
$P(2)$	881.575783(6)	26428977.084(187)	$R(49)$	915.991578(436)	27460736.676(****)
			$R(50)$	915.904717(280)	27458132.647(8390)

[a] The number in parentheses is the estimated 1-σ uncertainty.

venience, Table IV lists the calculated frequencies for the low J transitions that are most likely to be observed in similar hot band lasers. The frequencies and their estimated uncertainties were calculated with the constants in Table II (the fit without H terms) and the variance–covariance matrix in Table III. We have chosen to give the frequencies calculated without the H terms because extrapolation beyond the range of accurate measurements is less reliable when higher-order terms of questionable validity are included. On the other hand, the use of constants resulting from a lower-order fit usually gives overly optimistic estimates of the uncertainties of the extrapolated values. Because of this latter point, the users of Table IV are cautioned to remember that the calculated values of the frequencies beyond $J'' = 39$ have a reasonable probability of deviating from the true values by more than three times the estimated standard deviation. This is because the values extrapolated beyond $J'' = 39$ are susceptible to model errors (i.e., errors due to the truncated Hamiltonian), which are not taken into account in the statistical analysis that gives the estimated standard errors. Users are particularly cautioned not to use the constants in Table II to calculate transition frequencies for even higher J values than those given in Table IV.

The NBS Boulder authors acknowledge with appreciation the able assistance of D. J. Sukle, on sabbatical from Community College of Denver, who participated in the TDL phase of this work. We are also grateful to the Upper Atmospheric Research Office of NASA for partial support of this project.

References

1. F. R. Petersen, D. G. McDonald, J. D. Cupp, and B. L. Danielson, in *Laser Spectroscopy*, R. G. Brewer and A. Mooradian, Eds. (Plenum, New York, 1974, pp. 555–569.
2. C. Freed, L. C. Bradley, and R. G. O'Donnell, IEEE J. Quantum Electron. **QE-16,** 1195 (1980).
3. J. S. Wells, F. R. Petersen, and A. G. Maki, Appl. Opt. **18,** 3567 (1979).
4. J. S. Wells, F. R. Petersen, A. G. Maki, and D. J. Sukle, Appl. Opt. **20,** 1676 (1981).
5. C. Freed and A. Javan, Appl. Phys. Lett. **17,** 53 (1970).
6. B. G. Whitford, K. J. Siemsen, and J. Reid, Opt. Commun. **22,** 261 (1977).
7. F. R. Petersen, K. M. Evenson, D. A. Jennings, J. S. Wells, K. Goto, and J. J. Jimenez, IEEE J. Quantum Electron. **QE-11,** 838 (1975).
8. K. J. Siemsen, Opt. Lett. **6,** 114 (1981).
9. K. J. Siemsen, Opt. Commun. **34,** 447 (1980).
10. A. Baldacci, L. Linden, V. M. Devi, and K. N. Rao, J. Mol. Spectrosc. **72,** 135 (1978).
11. M. J. Reisfeld and H. Flicker, J. Mol. Spectrosc. **69,** 330 (1978).
12. A. G. Maki, E. K. Plyler, and R. J. Thibault, J. Res. Nat. Bur. Stand. Sect. A **67,** 219 (1963).
13. R. H. Wampler, J. Res. Nat. Bur. Stand. Sect. **B73,** 59 (1969).
14. J. Terrien, Metrologia **10,** 9 (1974).